Acta of Bioengineering and Biomechanics
Vol. 18, No. 4, 2016

Original paper
DOI: 10.5277/ABB-00444-2015-02

Computational and experimental model of electroporation for human aorta

NENAD FILIPOVIC[1]*, IGOR SAVELJIC[1], NEMANJA JOVICIC[2], IRENA TANASKOVIC[2], NEBOJSA ZDRAVKOVIC[2]

[1] Faculty of Engineering, University of Kragujevac, Kragujevac, Serbia.
[2] Faculty of Medical Sciences, University of Kragujevac, Kragujevac, Serbia.

Purpose: In this study the computational and experimental electroporation model with human aorta tissue is made in order to examine the reduction of smooth muscle cells. Methods. The segments in native state of the aorta are treated by electroporation method through a series of electrical impulses from 50 V/cm to 2500 V/cm. For each patient we analyzed one sample with and one sample without electroporation as a control. In the computational study, electrical field distribution is solved by the Laplace equation. The Pennes Bioheat equation without metabolism and blood perfusion heating is used to solve heat transfer problems. Different conductivity values are used in order to fit the experimental results. *Results:* Experimental histology has shown us that there are a smaller number of vascular smooth muscle cells (VSMC) nuclei at the tunica media, while the elastic fibre morphology is maintained 24 h after electroporation. In the computational model, heat generation coupled with electrical field is included. The fitting procedure is applied for conductivity values in order to make material properties of the aorta tissue. The fitting procedure gives tissue conductivity of 0.44 [S/m] for applied electrical field of 2500 V/cm. *Conclusions:* Future studies are necessary for investigation of a new device for in-vivo ablation with electroporation of plaque stenosis. It will open up a new avenue for stenosis treatment without stent implantation.

Key words: *electroporation, heat generation, ablation, VSMC reduction, fitting, conductivity*

1. Background

Electroporation is a non-linear biophysical process in which the application of pulsed electric fields leads to an increase in permeability of cells, through the creation of nanoscale pores in the lipid bilayer [2]. There is an increase in the conductivity throughout the electroporation pulse. Electroporation causes permeabilization of the cell membrane which increases the conductivity of the tissue. Irreversible electroporation (IRE) is an electrical field effect applied across a cell which destabilizes electric potential across the cell outer membrane and causes formation of permanent defects in the lipid bilayer. It causes permanent permeabilization of the cell membrane and leads to the changes in cell homeostasis and cell death [3], [6], [10]. Due to a very short duration, IRE could ablate substantial volumes of tissue without thermal effects [11].

Maor et al. [8] found that vascular smooth muscle cells (VSMC) nuclei begin to drop and that the number of VSMC nuclei in the arterial wall following IRE ablation is significantly lower compared to control arteries. They also found that the effect of VSMC decrease appears after seven days, when some cells are still visible and only apoptotic tests show that the cells are not alive. The decrease of the conductivity of tissue during sequential IRE is contradictory.

Sano et al. [12] investigated the ability to develop decellularized tissue scaffolds using non-thermal IRE on the organs undergoing active perfusion. Through histology, they have shown a density score improvement of 58.5 percent. Also, they found IRE threshold of 423 +/– 147 V/cm which may be used to predict the affected area.

Lackovic et al. [7] investigated the influence of tissue electrical conductivity and the parameters of elec-

* Corresponding author: Nenad Filipovic, University of Kragujevac, Sestre Janjica 6, 34000 Kragujevac, Serbia. Tel.: +381 34 334 379, e-mail: fica@kg.ac.rs

Received: August 17th, 2015
Accepted for publication: December 17th, 2015

tric pulses (amplitude, duration, number of pulses, pulse repetition frequency) on the temperature distribution within the tissue and the electrodes. Their results showed that, for the specific pulse parameters, at least locally, the tissue heating might be significant for electrochemotherapy, which is not critical, but for DNA electrotransfer it may be critical due to heating-related DNA damage or denaturation.

In this study, the ablation effect on the human aorta tissue during electroporation is investigated. The paper is organized as follows: firstly, in Section 2, the experimental and computational procedures for electroporation are presented, where the heat generation with electrical field is taken into account. In Section 3, the experimental and computational results are presented. In Section 4, the obtained results and potential tool for electroporation of plaque sites in the cardiovascular disease are described.

2. Methods

Histology procedure

Research samples were obtained during the autopsy of 35 male cadavers, 40 to 65 years old, who died from nonvascular disease. Time between sample acquisition from the cadavers and time of treatment was approximately 3 hours. The collection of samples was conducted at the Department of Pathology and Anatomical Diagnostics of the Clinical Center Kragujevac with the approval of the Ethics Committee of the Clinical Center Kragujevac. The Ethics Committee waived the need for consent from patients because the samples were taken from the Department of Pathology and Anatomical Diagnostics. The degree of atherosclerosis of the samples was determined according to the classification of the American Heart Association Committee on Vascular Lesions of the Council of Atherosclerosis [7]. All analyzed samples were in preatheroma stage (stage 3).

A 0.5 cm long and 0.5 cm wide segment from a plaque area of each artery was sampled. The segments in native state are treated by electroporation method with the device: ECM 399 electroporation system (BTX Harvard apparatus, Massachusetts, the United States), through a series of electrical impulses of low voltage (LV) of 50 LV to 500 LV and high voltage (HV) from 100 HV to 2500 HV, according to the following scheme (Tables 1 and 2). One electrode was placed on luminal part of tissue (tunica intima), while the other was placed on external part of the tissue (tunica adventitia). T is pulse length delivered to sample, ms is time constant for duration of pulse. One pulse was delivered during each voltage.

For each sample analyzed, one control sample of the same patient was used, without the leakage of electrical impulses.

Table 1. Low voltage (LV) from 50 V to 500 V

Ordinal number of the sample	Voltage	T	ms
1	50 LV	48,t	79 ms
2	100 LV	98,t	86 ms
3	150 LV	146,t	60 ms
4	200 LV	196,t	49 ms
5	250 LV	246,t	43 ms
6	300 LV	298,t	78 ms
7	350 LV	348,t	59 ms
8	400 LV	396,t	96 ms
9	450 LV	446,t	140 ms
10	500 LV	498,t	84 ms

Table 2. High voltage (HV) from 100 HV to 2500 HV

Ordinal number of the sample	Voltage	T	ms
11	100 HV	90,t	3 ms
12	200 HV	180,t	2 ms
13	300 HV	250,t	1 ms
14	400 HV	330,t	1 ms
15	500 HV	420,t	1 ms
16	600 HV	430,t	0 ms
17	700 HV	560,t	1 ms
18	800 HV	680,t	1 ms
19	900 HV	650,t	0 ms
20	1000 HV	780,t	1 ms
21	1100 HV	830,t	1 ms
22	1200 HV	900,t	1 ms
23	1300 HV	1000,t	1 ms
24	1400 HV	1100,t	1 ms
25	1500 HV	1110,t	1 ms
26	1600 HV	60,t	0 ms
27	1700 HV	80,t	0 ms
28	1800 HV	1340,t	0 ms
29	1900 HV	1480,t	0 ms
30	2000 HV	1400,t	0 ms
31	2100 HV	60,t	0 ms
32	2200 HV	110,t	0 ms
33	2300 HV	1720,t	0 ms
34	2400 HV	180,t	0 ms
35	2500 HV	80,t	0 ms

After electroporation procedure, the samples were prepared for analysis by light microscopy according to the standard procedure (2). The samples obtained

were fixed in 4% neutral buffered formalin solution, during 24 hours, at room temperature, dehydrated by the conduction through the series of alcohol of increasing concentration (70%, 96% and 100%), enlightened in xylene and embedded in paraffin.

The cross sections, 5 μm thick, were colored with Haematoxylin-eosin technique, according to the standard procedure [14].

The thickness of the intima and the media was measured using a standard Olympus BX51 microscope, at 100 times magnification. In each section, the measurement of the intima and the media thickness was applied on 10 evenly spaced visual fields. From the obtained data, the average thickness of these parameters was calculated for each sample.

The total number of the cells in the section was determined by the photomicrography of the whole cross-section with a small magnification (×20), by a specialized program NIH ImageJ.

The data obtained for each sample and its control are presented in tabular form.

Computational model

During electroporation pulse, electrical field distribution is solved by the Laplace equation

$$\nabla \cdot (\sigma \nabla \Phi) = 0 \tag{1}$$

where Φ is the electrical potential and σ is the electrical conductivity of the tissue. The solution of the Laplace equation yields the distribution of the potential within the tissue. The electric field is defined as the gradient of the potential

$$E = \nabla \Phi . \tag{2}$$

The heat generation rate per unit volume from the electric field (Joule heating, p) is defined as

$$p = \sigma |\nabla \Phi|^2 . \tag{3}$$

The Pennes Bioheat equation without metabolism and blood perfusion heating is used to solve heat transfer problems. Our Pennes Bioheat equation has the following form

$$\nabla \cdot (k \nabla T) + p = \rho c_p \frac{\partial T}{\partial t} \tag{4}$$

where k is the thermal conductivity of the tissue, T is the temperature, ρ is the tissue density, and c_p is the heat capacity of the tissue.

For each electrode configuration, the surface of one electrode is assumed to have a prescribed voltage, and the other electrode is set to the ground. The boundary condition of the tissue which is in contact with a charged electrode is defined as

$$\Phi = V_0 \tag{5}$$

where V_0 is the applied voltage and the electrical boundary condition at the interface of a grounded electrode and the tissue is defined as

$$\Phi = 0. \tag{6}$$

The boundaries where the analyzed domain is not in contact with an electrode are treated as electrically insulating

$$\frac{\partial \Phi}{\partial n} = 0. \tag{7}$$

Regarding the temperature boundary conditions, the boundary of the analyzed domain and the surfaces of the electrodes are considered to be adiabatic

$$\frac{\partial \mathbf{T}}{\partial n} = 0. \tag{8}$$

Due to electroporation and temperature, the conductivity changes were used to calculate the dynamic conductivity according to the following equation

$$\sigma = \sigma_0 [1 + f(E - E_0, E_1) + \alpha (T - T_0)] \tag{9}$$

where σ_0 is the baseline conductivity, f is a smoothed heaviside function with a continuous second derivative that ensures the numerical solution convergence. This function changes from zero to one when $E - E_0 = 0$ over the range E_1. E is the magnitude of the electric field, and E_0 is the magnitude of the electric field at which the transition occurs over the range, E_1. The baseline tissue conductivity was set to 0.067 S/m [1].

3. Results

The temperature distribution for three cases of different tissue conductivity σ = 0.1 S/m, 0.3 S/m and 0.5 S/m is presented in Fig. 1. This conductivity takes into account the temperature distribution from equation (9).

The voltage distribution for prescribed voltage on the electrode 600 V is shown in Fig. 2.

The electrical field distribution for applied electroporation 2500 V/cm is presented in Fig. 3. We used the values of the tissue heat capacity (c_p = 3.6 kJ·kg^{-1}K^{-1}), thermal conductivity (k = 0.512 W·m^{-1}K^{-1}) and density (ρ = 1050 kg·m^{-3}), taken from the literature [4], [13].

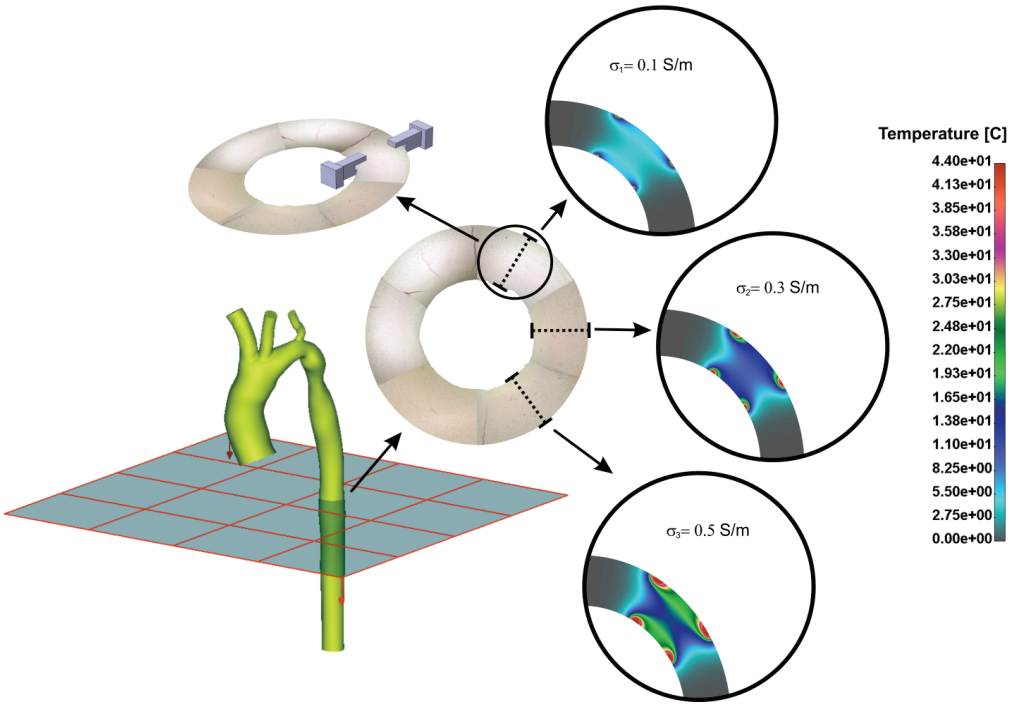

Fig. 1. Temperature distribution during electroporation with prescribed 2500 V/cm for three different tissue conductivities σ = 0.1 S/m, 0.3 S/m and 0.5 S/m

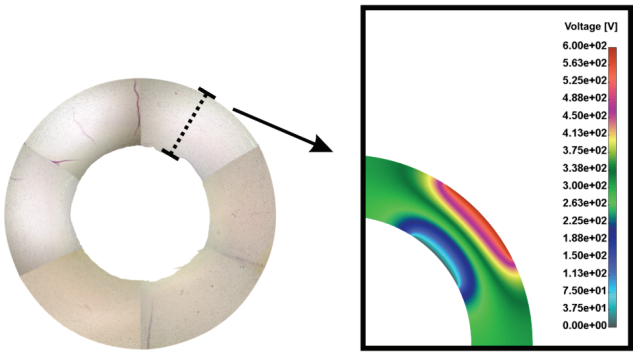

Fig. 2. Voltage distribution for applied electrode – 2500 V/cm

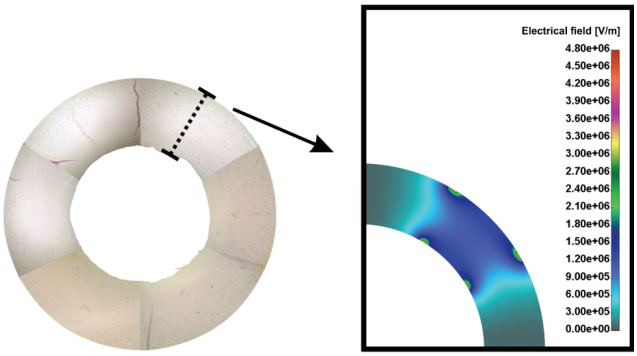

Fig. 3. Electrical field distribution for applied electroporation – 2500 V/cm

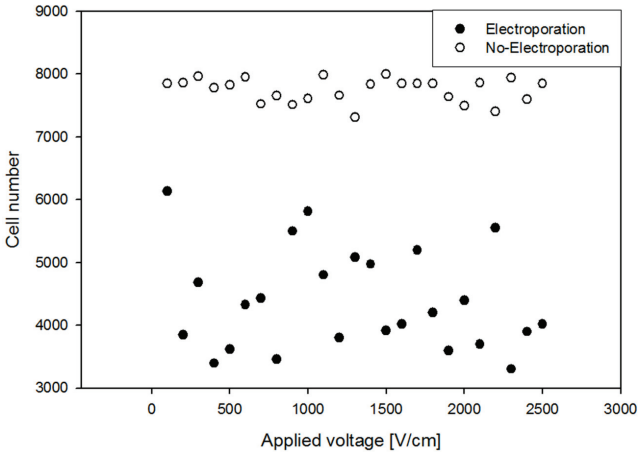

Fig. 4. Cell number distribution for differently applied voltages for tissue with and without electroporation

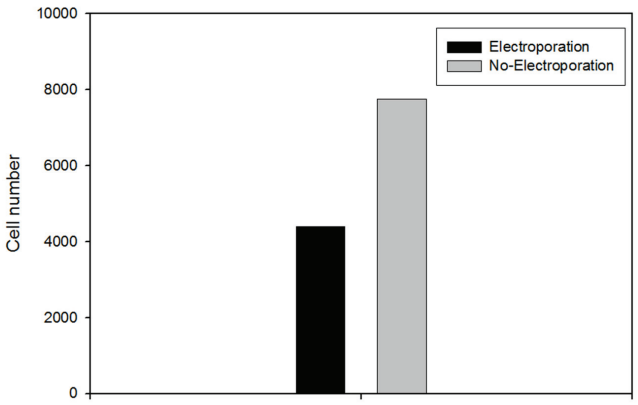

Fig. 5. Cell number for tissue with and without electroporation

The cell number distribution for differently applied voltages for tissue with and without electroporation is presented in Fig. 4. It can be seen that almost half of the cells died during electroporation effects. The cell number distribution is clearly shown in Fig. 5.

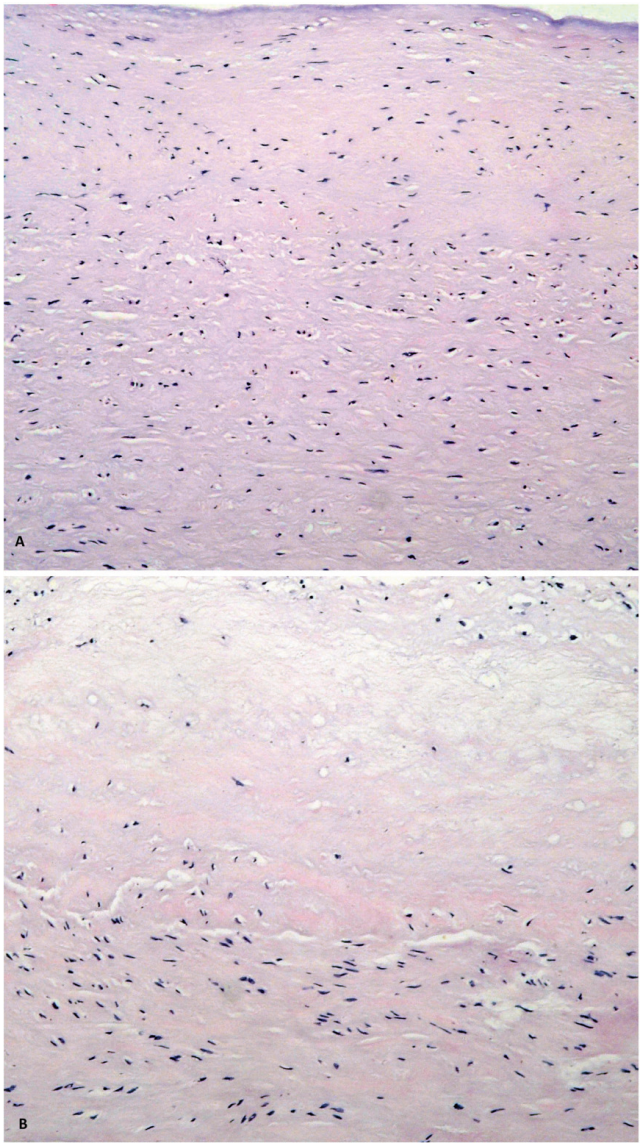

Fig. 6. Histology results: (a) tissue without electroporation; (b) tissue with electroporation

The histology results for tissue without and with electroporation are presented in Fig. 6. It can be observed that there are a smaller number of vascular smooth muscle cells nuclei at the tunica media. The elastic fiber morphology is maintained (Fig. 1).

Using computational simulation, we investigated to what extent ablation effects influenced the reduction of VSMC in the area where electroporation was implemented (Fig. 1). Three different tissue conductivities were used – 0.1, 0.3 and 0.5 [S/m] and the results are presented in Fig. 7. Also, experimental

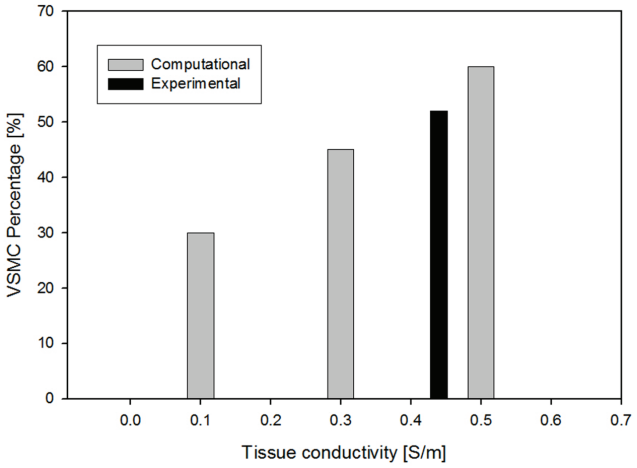

Fig. 7. Computational and experimental reduction of VSMC during electroporation procedure

results presented in black color in Fig. 7 are calculated from Figs. 4–6, 24 h after the electroporation procedure. It can be seen from experiment that there is a reduction of VSMC 50%. We connected VMSC apoptosis with thermal effect as temperature distribution more than 42 °C. The fitting tissue conductivity for the applied voltage of 600 V which corresponds to the applied electrical field of 2500 V/cm with 1 Hz frequency was 0.44 [S/m]. This conductivity corresponds to the experimental results for 50% VSMC reduction. For fitting procedure, we used simplex optimization method developed by John Nelder and Roger Mead [9]. This in a non-gradient optimization method, it involves only function evaluations (no derivatives).

4. Conclusions

By using electroporation, the human aorta tissue was tested in order to examine the reduction of smooth muscle cells. A 0.5 cm long and 0.5 cm wide segment from a plaque area of each artery was sampled. The segments in native state were treated by electroporation method through a series of electrical impulses of low voltage (LV) of 50 LV to 500 LV and high voltage (HV) from 100 HV to 2500 HV. For each sample analyzed, one control sample of the same age was used, without the leakage of electrical impulses.

We have developed the computational model for electroporation experimental process. Electrical field distribution is solved by the Laplace equation. The heat generation is coupled with electrical field through

Joule heating. The Pennes Bioheat equation is used to solve heat transfer problems.

For each electrode configuration, the surface of one electrode was assumed to have a prescribed voltage, and the other electrode was set to the ground. The conductivity changes due to electroporation and temperature were used to calculate the dynamic conductivity. Different conductivity values were used in order to fit experimental results.

Experimental histology pictures clearly show that there is smaller number of vascular smooth muscle cells (VSMC) nuclei at the tunica media while the elastic fiber morphology is maintained.

We included heat generation coupled with electrical field because electroporation of the aorta blood vessel ablates all the cells to the margin, including VSMC. It seems that electroporation pulses do not compromise the blood vessel matrix. The fitting procedure for obtaining tissue conductivity for applied electrical field of 2500 V/cm calculated the value of 0.44 [S/m]. Future studies will be continued in the direction of examining a new device for in-vivo ablation with electroporation of plaque stenosis. Obviously, the reduction of VSMC may be a trigger for the plaque decrease and therefore the reduction of the stenosis. This will open a new avenue for stenosis treatment without stent implantation. Further study is necessary for very precise and optimal design of the device for electroporation as well as computational models which take into account a patient specific anatomy.

Acknowledgments

This study was funded by grants from the Serbian Ministry of Education, Science and Technological Development III41007 and ON174028.

Reference

[1] BANCROFT J.D., GAMBLE M., *Theory and practice of histological techniques*, 5th ed., Churchill Livingstone, Edinburgh, London, New York, Oxford, 2002.

[2] DAVALOS R., MIR L., RUBINSKY B., *Tissue ablation with irreversible electroporation*, Annals Biomed. Eng., 2005, 33, 223–231.

[3] DENG Z.S., LIU J., *Blood Perfusion-Based Model for Characterizing the Temperature Fluctuations in Living Tissue*, Phys. A STAT Mech. Appl., 2001, 300, 521–530.

[4] DUCK F.A., *Physical Properties of Tissues: A Comprehensive Reference Book*, San Diego, Academic Press, 1990.

[5] EDD J.F., DAVALOS R.V., *Mathematical Modeling of Irreversible Electroporation for Treatment Planning*, Technology in Cancer Research and Treatment, ISSN 1533-0346, August 2007, 6(4).

[6] HAMILTON W.A., SALE J.H., *Effects of high electrical fields on microorganisms. II. Mechansims of action of the lethal effect*, Biochimica et Biophysica Acta, 1967, 148, 789–800.

[7] LACKOVIC I., MAGJAREVIC R., MIKLAVCIC D., *Three-dimensional Finite-element Analysis of Joule Heating in Electrochemotherapy and in vivo Gene Electrotransfer*, IEEE Transactions on Dielectrics and Electrical Insulation, 2009, 16(5), 1338–1347.

[8] MAOR E., IVORRA A., LEOR J., RUBINSKY B., *The Effect of Irreversible Electroporation on Blood Vessels*, Technology in Cancer Research and Treatment, ISSN 1533-0346, August 2007, 6(4), 307–312.

[9] NELDER J., MEAD R., *A simplex method for function minimization*, Computer Journal, 1965, 7, 308–313.

[10] SALE A.J.H., HAMILTON W.A., *Effects of high electri fields on microorganisms III. Lysis of erythrocytes and protoplasts*, Biochimica et Biophysica Acta, 1968, 163, 37–43.

[11] SALE J.H., HAMILTON W.A., *Effects of high electrical fields on microorganisms. I. Killing of bacteria and yeast*, Biochimica and Biophysisca Acta, 1967, 148, 781–788.

[12] SANO M.B., NEAL R.E., GARCIA P.A., GERBER D., ROBERTSON J., DAVALOS RV., *Towards the creation of decellularized organ constructs using irreversible electroporation and active mechanical perfusion*, BioMedical Engineering OnLine, 2010, 9: http://www.biomedical-engineering-online.com/content/9/1/83 (2010).

[13] SEL D., CUKJATI D., BATIUSKAITE D., SLIVNIK T., MIR L.M., MIKLAVCIC D., *Sequential Finite Element Model of Tissue Electropermeabilization*, IEEE Trans. Biomed. Eng., 2005, 52, 816–827.

[14] STARY H.C., CHANDLER A.B., DINSMORE R.E., FUSTER V., GLAGOV S., INSULL W.Jr., ROSENFELD M.E., SCHWARTZ C.J., WAGNER W.D., WISSLER R.W., *A definition of advanced types of atherosclerotic lesions and a histological classification of atherosclerosis, American Heart Association*, A report from the Committee on Vascular Lesions of the Council on Arteriosclerosis, Circulation, 1995, 92, 1355–1374.